

See discussions, stats, and author profiles for this publication at: <https://www.researchgate.net/publication/228361087>

Modeling the Water–Supercritical CO₂ Partition Coefficients of Organic Solutes Using a Linear Solvation Energy Relationship †

ARTICLE *in* THE JOURNAL OF PHYSICAL CHEMISTRY B · FEBRUARY 1998

Impact Factor: 3.3 · DOI: 10.1021/jp973047o

CITATIONS

23

READS

22

2 AUTHORS:



[Anthony Lagalante](#)

Villanova University

57 PUBLICATIONS 750 CITATIONS

[SEE PROFILE](#)



[Thomas J Bruno](#)

National Institute of Standards and Technolo...

198 PUBLICATIONS 3,976 CITATIONS

[SEE PROFILE](#)

Modeling the Water-R134a Partition Coefficients of Organic Solutes Using a Linear Solvation Energy Relationship

Anthony F. Lagalante, Adam M. Clarke, and Thomas J. Bruno*

National Institute of Standards and Technology, Physical and Chemical Properties Division 838.01,
325 Broadway, Boulder, Colorado 80303

Received: June 23, 1998; In Final Form: August 17, 1998

The water-R134a partition coefficients for a set of 11 organic solutes have been measured using a high-pressure, spectroscopic technique. Water partition coefficients of the organic solutes were measured in the gas and supercritical phases of R134a. A linear solvation energy relationship (LSER) was developed to predict the measured water-R134a partition coefficients using the Kamlet–Taft descriptors of the solute and solvent molecules as independent variables. Considering the entire water-R134a partition coefficient data, the LSER model has an average absolute relative deviation of 30%. Only considering the data above the critical density of R134a, the LSER has an average absolute relative deviation of 17.5%.

Introduction

A number of papers have been published dealing with the predictive capability of a linear solvation energy relationship (LSER) as applied to partitioning between water and an immiscible, or partially miscible, organic solvent.^{1–6} Methods for the reliable prediction of water–solvent partition coefficients are especially important in the fields of pharmaceutical research and wastewater cleanup. With the production phase-out of chlorinated solvents, as mandated by the Montreal Protocol, interest in alternative solvent technology has grown significantly. In many industrial applications, supercritical fluids are being evaluated as replacements for chlorinated solvents, and the need for a systematic approach to replacement is great. At present, LSERs have been used to predict solid–fluid enhancement factors for supercritical CO₂ systems⁷ and retention factors in supercritical fluid chromatography.⁸

Recently, we reported a model for a published set of water–CO₂ partition coefficients for six organic solutes using a LSER.⁹ The data set used in the LSER model was limited to only six solutes, and therefore a more extensive set of water–supercritical fluid partition coefficients were modeled to ascertain the utility of the LSER method. In this study, the partitioning from water into 1,1,1,2-tetrafluoroethane (R134a) was measured. R134a is currently widely used as a fluid in commercial automotive and household refrigeration devices. The critical temperature (101.1 °C) is significantly higher than that of CO₂, while the critical pressure (4.06 MPa) is significantly lower than that of CO₂. In contrast to CO₂, R134a possesses a permanent dipole moment (2.06 D) which is beneficial for dissolving polar solutes.¹⁰ The physical properties of fluorocarbon-based solvents suggest that they are superior supercritical fluid extraction solvents when compared to CO₂.¹¹ In this paper, we will demonstrate that the LSER approach is also amenable to modeling the water-R134a partition coefficients of a set of organic solutes.

LSER Approach. As shown by Abraham,⁵ water–solvent partition coefficients, K , are reliably modeled using five solute

descriptors: the excess index of refraction R_2 , the dipolarity/polarizability π_2^H , the effective hydrogen bond acidity α_2^H , the effective hydrogen bond basicity β_2^H , and McGowan's¹² intrinsic volume V_2 . The general form of the LSER is

$$\log K = C_1 + C_2 R_2 + C_3 \pi_2^H + C_4 \alpha_2^H + C_5 \beta_2^H + C_6 V_2 \quad (1)$$

where C_i are the coefficients of the linear regression. The partition coefficients in this study are defined as the ratio of the concentration (mol L⁻¹) of the solute in the organic phase to the concentration (mol L⁻¹) of the solute in the aqueous phase. These coefficients represent vectors, each having a magnitude and direction in relationship to the equilibrium property of the system that is being modeled.

In partition coefficient modeling between water and conventional organic solvents, the solvent descriptors are not generally included in the LSER equation. Rather, a separate LSER is generated for each organic solvent considered. This approach is valid for modeling partition coefficients in conventional organic solvents because the solvent descriptors are not variable at ambient temperature and pressure and therefore will be accounted for in the LSER constant term. Supercritical fluids, however, have a tunable solvent strength as evidenced by the density-dependent dipolarity/polarizability of the solvent π_1 .^{13–16} Therefore, it is expected that any derived LSER approach for supercritical fluids would require additional density-dependent solvent terms.

In a recent paper, we measured π_1 for six fluorinated ethanes including R134a.¹⁷ The π_1 values for R134a can be fitted to a cubic polynomial in R134a density given by

$$\pi_1 = 1.191 + 0.4266\rho_{\text{R134a}} - 0.05473\rho_{\text{R134a}}^2 + 0.002514\rho_{\text{R134a}}^3 \quad (2)$$

where ρ_{R134a} , expressed in mol L⁻¹, is the density of the pure solvent calculated using an extended corresponding states method with R134a as a reference fluid.¹⁸ Equation 2 was determined at temperatures of 30, 105, and 120 °C; π_1 was found to be insensitive to temperature over the density range investigated (0–12 mol L⁻¹). The π_1 values sharply inflect at the

* To whom correspondence should be addressed. FAX 303-497-5224, e-mail bruno@boulder.nist.gov.

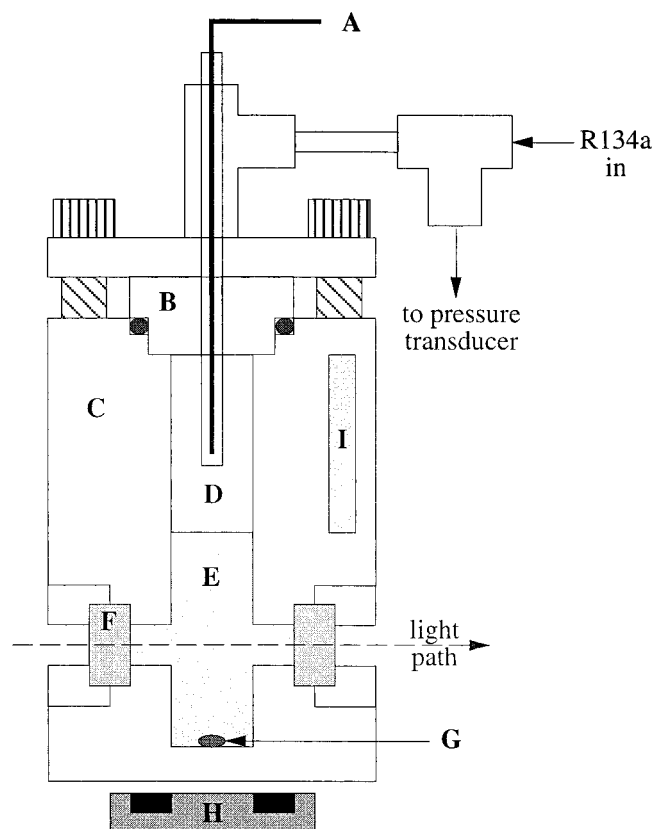


Figure 1. Spectroscopic cell for determination of water-R134a partition coefficients: A, J-type thermocouple; B, stainless steel plug; C, stainless steel cell body; D, R134a; E, organic solute in water; F, quartz window; G, magnetic stirring bar; H, NdFeB magnets on fan motor; I, internal platinum resistance thermometer.

critical density of R134a (5.05 mol L^{-1}) and extrapolate to the gas-phase value of the solvatochromic probe.

Experimental Section

Chemicals. R134a (99.9% purity), benzoic acid (99% purity), benzyl alcohol (99% purity), caffeine (99% purity), 4-chloroaniline (98% purity), cyclohexanone (99.9% purity), 2-hexanone (98% purity), 4-methyl-2-pentanone (99.5% purity), 4-nitroaniline (99% purity), 2-nitrophenol (98% purity), phenol (98% purity), and 4-*tert*-butyl phenol (99% purity) were obtained from commercial suppliers and were used as received. Water was distilled and deionized prior to use.

Spectroscopic Cell. The water-R134a partition coefficients of the solutes studied were measured using the high-pressure spectroscopic cell in Figure 1. Details of the spectroscopic cell design were previously reported,¹⁹ and therefore only modifications on the cell for this work will be described here. A stainless steel plug was installed to provide a sealing surface for the poly(tetrafluoroethylene) O-ring at the cell top. On top of this plug, a stainless steel tee was attached, and a stainless steel tube containing a J-type thermocouple was fed through one arm of the tee into the cell cavity. The glass-to-metal seal on the faces of the quartz windows was made using polyether ether ketone washers.

Partition Coefficient Measurement. For each organic solute, solutions of known molarity were prepared by weighing a quantity of the solute into a volumetric flask and diluting with distilled, deionized water. These solutions were diluted until the absorbance at the UV-peak maximum was in the range 1.0–1.5 absorbance units. At room temperature, 5 mL of the

aqueous organic solute was volumetrically pipetted into the bottom of the cell. The top of the cell was sealed, and care was taken to ensure that the light path through the quartz windows was unobstructed by any trapped air bubbles. An initial absorbance spectrum was measured using a UV-vis photodiode array spectrophotometer that had a resolution of 2 nm. The cell was quickly flushed with gaseous R134a and heated to 110°C by four internal 100 W cartridge heaters. The current to the cartridge heaters was regulated by a microprocessor-based temperature controller that monitored a platinum resistance thermometer (PRT) located within the stainless steel cell wall. The fluid was mixed by a poly(tetrafluoroethylene)-coated stirring bar that was coupled to external NdFeB magnets mounted on top of a fan motor. When the temperature had stabilized, the cell was pressurized with R134a using a syringe pump. Although the temperature measured by the PRT was nominally $110 \pm 0.2^\circ\text{C}$ during all experiments, the interior temperature of the cell, as measured by the internal J-type thermocouple, showed considerable deviations (approximately $\pm 2^\circ\text{C}$) from the 110°C set point. The temperature reading from the internal thermocouple, rather than the PRT temperature, was regarded as a truer indicator of the system temperature because the thermocouple was in better thermal contact with the internal contents of the cell. Pressure within the cell was measured by a resonating quartz crystal transducer that had a range of 0–68 MPa and an accuracy of $\pm 680 \text{ Pa}$. Radiation from the spectrophotometer was passed only through the aqueous-phase portion of the cell to ascertain when an equilibrium partitioning had been achieved. When a constant absorbance was obtained, the absorbance was recorded at the UV-peak maximum as well as the pressure and temperature of the system. Pressure in the cell was then increased to obtain representative intervals of the R134a density over the isotherm.

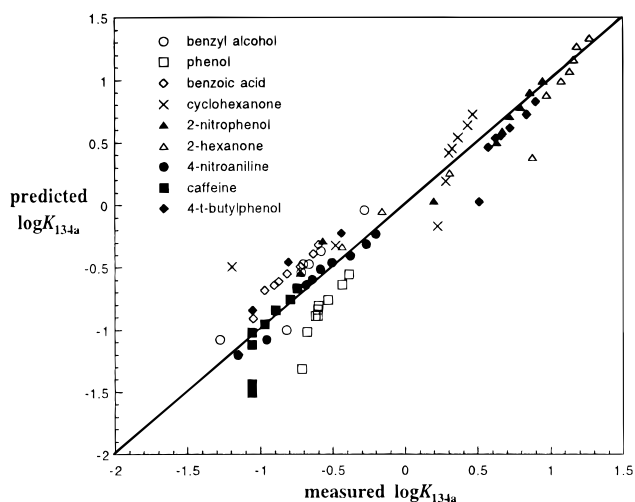
Results

Partition Coefficient Data. Equilibrium within the cell was typically reached within 20 min, although for some of the solutions it was necessary to wait up to 1.5 h between data points. The molar absorptivity of the organic solute was calculated from the Beer–Lambert law using the measured absorbance value at the UV-peak maximum and the known molarity of the aqueous solution. For every solute studied, the wavelength maximum of the UV peak remained constant from the initial absorbance reading to the highest pressure studied. The number of moles of solute that were transferred into the R134a phase was calculated from the decrease in absorption of the UV peak, and using the internal cell volume with the stirbar present (10.35 mL), the concentration in mol L^{-1} of the organic solute in R134a phase was calculated. The partition coefficient was determined by calculating the ratio of the molar concentration of organic solute in the R134a phase to the molar concentration of the organic solute in the aqueous phase. Table 1 lists the experimentally determined $\log K_{\text{R134a}}$ values for the 11 solutes studied and the temperature, pressure, and density of pure fluid R134a at each measurement. The relative standard uncertainty in the water-R134a partition coefficient measurement was 2%.

LSER Modeling. Table 2 lists the solute descriptors that were used as the independent variables in the water-R134a partition coefficient LSER.^{5,7,20,21} Although the reported solute descriptors were measured at 25°C , we have assumed that the values, relative to each other, remain constant up to 110°C . Additionally, the dipolarity/polarizability descriptor of R134a calculated using eq 2 was used in the LSER. Using these five

TABLE 1: Partition Coefficients of the Organic Solutes Studied

T (°C)	p (MPa)	ρ_{R134a} (mol L ⁻¹)	log K_{R134a}	T (°C)	p (MPa)	ρ_{R134a} (mol L ⁻¹)	log K_{R134a}
Benzoic Acid							
111.7	4.43	2.94	-1.15	111.0	7.14	8.02	-0.81
111.8	4.78	4.10	-1.05	110.0	9.31	8.77	-0.72
109.4	4.91	5.82	-0.97	110.3	15.70	9.74	-0.63
111.0	5.30	6.43	-0.90	109.1	20.19	10.20	-0.60
112.2	5.74	6.89	-0.87				
Benzyl Alcohol							
108.6	4.23	2.79	-1.28	108.8	5.02	6.41	-0.70
110.5	4.41	3.03	-0.82	112.4	5.45	6.40	-0.66
108.1	4.59	4.52	-0.75	108.7	7.06	8.19	-0.58
110.2	4.92	5.53	-0.72	111.6	29.21	10.73	-0.28
Caffeine							
111.4	4.50	3.13	-1.06	110.4	5.97	7.40	-0.97
113.0	4.67	3.41	-1.06	110.6	10.59	9.00	-0.89
110.0	4.83	5.13	-1.06	111.1	15.97	9.74	-0.79
110.9	5.19	6.21	-1.06	109.9	21.68	10.29	-0.74
Cyclohexanone							
111.0	3.83	2.03	-1.19	110.4	5.96	7.39	0.32
113.1	4.23	2.46	-0.48	110.9	9.36	8.73	0.37
112.7	4.46	2.90	0.23	111.4	15.05	9.62	0.43
111.9	4.85	4.44	0.28	110.4	20.95	10.22	0.47
110.5	5.40	6.74	0.30				
4-Nitroaniline							
110.3	4.24	2.66	-1.15	110.3	6.92	7.98	-0.51
110.3	4.41	3.04	-0.96	112.2	9.83	8.76	-0.38
110.2	4.89	5.37	-0.68	111.6	15.17	9.63	-0.27
111.6	5.12	5.78	-0.64	111.5	20.86	10.17	-0.20
110.0	5.57	7.07	-0.59				
2-Nitrophenol							
107.1	3.03	1.39	-0.72	109.9	5.87	7.39	0.72
110.6	3.71	1.92	-0.57	110.0	8.30	8.51	0.79
110.8	4.30	2.73	0.20	110.6	15.24	9.68	0.86
110.1	4.78	4.79	0.63	109.9	21.33	10.26	0.95
111.9	5.10	5.60	0.67				
4-Chloroaniline							
106.8	3.78	2.13	-1.05	110.5	5.90	7.33	0.21
113.2	4.41	2.75	-0.37	110.5	6.98	7.99	0.26
110.5	4.73	4.32	0.08	110.1	11.58	9.20	0.31
110.5	5.18	6.30	0.13	111.0	17.18	9.87	0.37
110.6	5.47	6.82	0.17	112.0	21.45	10.21	0.42
2-Hexanone							
110.5	2.69	1.13	-0.43	112.3	5.31	6.11	1.08
109.0	3.40	1.66	-0.16	109.6	5.85	7.40	1.13
110.2	4.06	2.37	0.31	110.2	9.46	8.79	1.16
113.6	4.40	2.71	0.88	111.6	16.22	9.74	1.18
110.4	4.83	4.93	0.98	113.3	21.81	10.19	1.27
4-Methyl-2-pentanone							
110.9	1.83	0.69	-0.49	110.6	5.34	6.61	1.15
110.5	3.19	1.46	-0.10	111.5	5.84	7.12	1.20
111.3	3.67	1.86	0.13	110.8	8.49	8.51	1.25
112.2	4.23	2.51	0.59	113.3	15.91	9.65	1.34
111.0	4.69	3.92	0.95	113.6	21.44	10.15	1.42
111.1	5.03	5.60	1.08				
Phenol							
112.2	4.61	3.35	-0.71	108.6	5.98	7.63	-0.60
110.6	4.83	4.88	-0.68	110.4	7.94	8.37	-0.53
111.1	5.21	6.21	-0.62	107.6	13.93	9.64	-0.44
113.5	5.50	6.22	-0.60	111.0	20.73	10.18	-0.39
110.2	5.58	7.05	-0.60				
4- <i>t</i> -Butylphenol							
107.2	2.64	1.13	-1.05	108.9	5.34	6.98	0.62
108.7	3.62	1.88	-0.81	110.1	5.88	7.36	0.66
111.7	4.16	2.43	-0.44	110.9	8.09	8.38	0.72
112.0	4.55	3.20	0.51	113.2	14.80	9.52	0.84
109.6	4.93	5.82	0.57	112.9	21.67	10.19	0.90

**Figure 2.** Comparison of measured water-R134a partition coefficients and those predicted by the LSER of eq 3.**TABLE 2: Solute Descriptors Used in the LSER Model**

solute	R_2	π_2^H	α_2^H	β_2^H	V_2
benzoic acid	0.730	0.90	0.59	0.40	0.932
benzyl alcohol	0.803	0.87	0.33	0.56	0.916
caffeine	1.500	1.60	0.00	1.35	1.363
4-chloroaniline	1.060	1.13	0.30	0.31	0.939
cyclohexanone	0.403	0.86	0.00	0.56	0.861
2-hexanone	0.136	0.68	0.00	0.51	0.970
4-methyl-2-pentanone	0.111	0.65	0.00	0.51	0.970
4-nitroaniline	1.22	1.91	0.42	0.38	0.991
2-nitrophenol	1.015	1.05	0.05	0.37	0.949
phenol	0.805	0.89	0.60	0.30	0.775
4- <i>tert</i> -butyl phenol	0.81	0.89	0.56	0.41	1.339

solute descriptors and one solvent descriptor, the following LSER was found:

$$\log K_{R134a} = -0.4778R_2 - 0.3164\pi_2^H - 2.512\alpha_2^H - 2.587\beta_2^H + 2.778V_2 + 1.841\pi_1 \quad (3)$$

$$n = 102, \quad r = 0.964, \quad kSD = 0.409, \quad \% \text{ AARD} = 30.03$$

The percentage average absolute relative deviation (% AARD) in predicting the measured K_{R134a} values, the correlation coefficient of the regression r , and the standard deviation SD, of the LSER equation multiplied by a coverage factor, $k = 2$, are also reported.²²

Figure 2 illustrates the correlation between the predicted and measured values of the water-R134a partition coefficient. Equilibrium data below the critical point of a solvent are not of great practical interest since the solubilities of solutes are typically much higher above the critical point of the solvent. Considering only the portion of the partition coefficient data above the critical density of R134a, the LSER can be reevaluated to give

$$\log K_{R134a} = -0.4078R_2 - 0.3742\pi_2^H - 2.593\alpha_2^H - 2.777\beta_2^H + 2.884V_2 + 1.955\pi_1 \quad (4)$$

$$n = 70, \quad r = 0.961, \quad kSD = 0.294, \quad \% \text{ AARD} = 17.45$$

The standard errors of the coefficients in the LSER equations (3) and (4) are listed in Table 3.

Discussion

In contrast to the water-CO₂ partition coefficients of a set of six organic solutes, the data set examined in this study is

TABLE 3: Standard Errors of the LSER Coefficients

variable	eq 3	eq 4	variable	eq 3	eq 4
R_2	0.0962	0.0865	β_2^H	0.1273	0.1065
π_2^H	0.0949	0.0817	V_2	0.1005	0.0827
α_2^H	0.1203	0.0993	π_1	0.0962	0.1407

sufficiently large to draw some conclusions about the form of the LSER chosen. The use of a separate term to account for the tunable dipolarity/polarizability of the solvent yields a better predictive ability than using a solvent–solute cross term, such as $\pi_2^H\pi_1$. Equation 3 can predict the water–R134a partition coefficient with an AARD of 30%. This uncertainty is comparable to equation of state modeling incorporating an empirical binary interaction coefficient. To model water partitioning, additional interaction parameters would be necessary since the supercritical phase is a ternary, as opposed to a simpler binary, mixture composed of fluid, water, and the organic solute. Modeling approaches for supercritical fluids, including equation of state modeling, often rely on physical constants of the solute and solvent that are difficult to obtain. When unavailable, physical constants (solute critical point data or solute vapor pressure) are often estimated using empirical relationships. The LSER approach to modeling equilibrium in supercritical fluids offers a simpler alternative to equation of state modeling and is as reliable in its predictive ability. The true advantage of the LSER approach is that equilibria for other solutes, with known solute descriptors, can be predicted without having to optimize additional adjustable parameters for the new system.

Equations 3 and 4 indicate that the same solute descriptors used to model partition coefficients between water and conventional organic solvents are applicable to modeling water–supercritical fluid partition coefficients. This is likely to be a consequence of the fact that, in both organic solvent extraction and supercritical fluid extraction, the majority of the thermodynamic nonideality resides with the solute in the aqueous phase. While the solute may not exactly exhibit ideal behavior in an organic solvent or R134a, the nonidealities in these phases will be smaller than the aqueous-phase nonidealities. Water has a reported maximum solubility of 0.83 % percent in R134a at 110 °C, 34.48 MPa,²³ and may alter the dipolarity/polarizability of the R134a phase. The model presented in this study may be improved by the incorporation of a density-dependent mixing term to account for the dipolarity/polarizability of water in the R134a phase; however, the predictive ability, especially above the critical density of R134a, is already within an acceptable error for measurements in supercritical fluids.

The coefficients of eqs 3 and 4 should be related to the differences between the water and R134a solvent descriptors. The presence of π_1 in eqs 3 and 4 may be due either to its direct contribution to the partition coefficient or to its association with the ρ_{P134a} term. It is not surprising that the coefficient of

π_1 is positive, because the increase in polarizability, and therefore density, usually results in increased solvent strength. The dipolarity/polarizability of the solute plays a less important, yet still statistically significant, role in the ability of a solute to partition into the supercritical phase. The coefficients of eqs 3 and 4 indicate that the measured partition coefficients strongly depend on the dipolarity/polarizability of R134a as well as the solute volume, hydrogen bond donor ability, and hydrogen bond acceptor ability. The hydrogen bond acceptor ability of R134a is approximately zero according to our measurements,¹⁷ and therefore the coefficient associated with α_2^H is expected to be negative as R134a will not interact with strong hydrogen bond donor solutes. The success of this model suggests that other types of equilibrium processes in supercritical fluids may be reliably modeled using a LSER and that the nonidealities of the supercritical fluid state may be better described using empirical solvent descriptors instead of equation of state modeling.

Acknowledgment. A.F.L. acknowledges the Professional Research Experience Program at the National Institute of Standards and Technology.

References and Notes

- (1) Meyer, P.; Maurer, G. *Ind. Eng. Chem. Res.* **1993**, 32, 2105.
- (2) Meyer, P.; Maurer, G. *Ind. Eng. Chem. Res.* **1995**, 34, 373.
- (3) Kamlet, M. J.; Doherty, R. M.; Abraham, M. H.; Marcus, Y.; Taft, R. W. *J. Phys. Chem.* **1988**, 92, 5244.
- (4) Kamlet, M. J.; Doherty, R. M.; Carr, P. W.; Mackay, D.; Abraham, M. H.; Taft, R. W. *Environ. Sci. Technol.* **1988**, 22, 503.
- (5) Abraham, M. H.; Chadha, H. S.; Whiting, G. S.; Mitchell, R. C. *J. Pharm. Sci.* **1994**, 83, 1085.
- (6) Kamlet, M. J.; Doherty, R. M.; Abboud, J. M.; Abraham, M. H.; Taft, R. W. *CHEMTECH* **1986**, 16, 566.
- (7) Bush, D.; Eckert, C. A. In *ACS Symposium Series on Supercritical Fluid Extraction*; Abraham, M., Sunol, A., Eds.; American Chemical Society: Washington, DC, 1997; Vol. 670, p 37.
- (8) Weckwerth, J. D.; Carr, P. W. *Anal. Chem.* **1998**, 70, 1404.
- (9) Lagalante, A. F.; Bruno, T. J. *J. Phys. Chem. B* **1998**, 102, 907.
- (10) Bruno, T. J. *Handbook for the Analysis and Identification of Alternative Refrigerants*; CRC Press: Boca Raton, FL, 1995.
- (11) Roth, M. *Anal. Chem.* **1996**, 68, 4474.
- (12) Abraham, M. H.; McGowan, J. C. *Chromatographia* **1987**, 23, 243.
- (13) Sigman, M. E.; Lindley, S. M.; Leffler, J. E. *J. Am. Chem. Soc.* **1985**, 107, 1471.
- (14) Smith, R. D.; Frye, S. L.; Yonker, C. R.; Gale, R. W. *J. Phys. Chem.* **1987**, 91, 3059.
- (15) Yonker, C. R.; Smith, R. D. *J. Phys. Chem.* **1988**, 92, 235.
- (16) Engel, T. M.; Olesik, S. V. *Anal. Chem.* **1991**, 63, 1830.
- (17) Lagalante, A. F.; Hall, R. L.; Bruno, T. J. *J. Phys. Chem. B* **1998**, 102, 6601.
- (18) Huber, M. L.; Ely, J. F. *Int. J. Refrig.* **1994**, 17, 18.
- (19) Hansen, B. N.; Lagalante, A. F.; Sievers, R. E.; Bruno, T. J. *Rev. Sci. Instrum.* **1994**, 65, 2112.
- (20) Abraham, M. H. *Chem. Soc. Rev.* **1993**, 22, 73.
- (21) Abraham, M. H.; Haftvan, J. A.; Whiting, G. S.; Leo, A. *J. Chem. Soc., Perkin Trans.* **1994**, 2, 1777.
- (22) Taylor, B. N.; Kuyatt, C. E. *Guidelines for Evaluating and Expressing the Uncertainty of NIST Measurement Results*, National Institute of Standards and Technology: Washington, DC, 1994; Tech. Note 1297.
- (23) Jackson, K.; Bowman, L. E.; Fulton, J. L. *Anal. Chem.* **1995**, 67, 2368.